Production of doubly charmed hadrons Ξ_{cc}^{++} and T_{cc}^{+} in relativistic heavy-ion collisions

Baoyi Chen,[1,*] Meimei Yang,[1,†] Ge Chen,[2,‡] Jiaxing Zhao,[3,§] and Xiao-hai Liu[1,‖]
[1]*Department of Physics, Tianjin University, Tianjin 300350, China*
[2]*Department of Physics and Astronomy, UCL, Gower Street, London WC1E 6BT, England*
[3]*SUBATECH, Université de Nantes, IMT Atlantique, IN2P3/CNRS, 4 Rue Alfred Kastler, 44307 Nantes Cedex 3, France*

(Received 10 September 2023; revised 5 May 2024; accepted 16 May 2024; published 11 June 2024)

Heavy-ion collisions provide a unique opportunity for studying the properties of exotic hadrons with two charm quarks. The production of T_{cc}^{+} is significantly enhanced in nuclear collisions compared to proton-proton collisions due to the creation of multiple-charm pairs. In this study, we employ the Langevin equation in combination with the instantaneous coalescence model (LICM) to investigate the production of T_{cc}^{+} and Ξ_{cc}^{++} which consists of two charm quarks. We consider T_{cc}^{+} as molecular states composed of D and D^{*} mesons. The Langevin equation is used to calculate the energy loss of charm quarks and D mesons in the hot medium. The hadronization process, where charm quarks transform into each D state as constituents of T_{cc}^{+} production, is described using the coalescence model. The coalescence probability between D and D^{*} is determined by the Wigner function, which encodes the information of the T_{cc}^{+} wave function. Our results show that the T_{cc}^{+} production varies by approximately 1 order of magnitude when different widths in the Wigner function, representing distinct binding energies of T_{cc}^{+}, are considered. This variation offers valuable insights into the nature of T_{cc}^{+} through the analysis of its wave function. Ξ_{cc}^{++} is treated as a hadronic state produced at the hadronization of the deconfined matter. Its production is also calculated as a comparison with the molecular state T_{cc}^{+}.

DOI: 10.1103/PhysRevC.109.064909

I. INTRODUCTION

The understanding of hadron properties is deeply rooted in nonperturbative quantum chromodynamics (QCD), which governs the confinement of fundamental quarks and gluons. In the field of particle physics, the investigation of exotic hadrons has gained significant importance. Exotic hadrons challenge our understanding of the quark model and provide insights into the strong interaction dynamics within QCD [1–8]. Recently, the LHCb Collaboration made a remarkable observation of the doubly charmed state T_{cc}^{+} [9,10]. This discovery sparked debates regarding the nature of multicharm states, such as X(3872) and T_{cc}^{+}, which are believed to be either compact tetraquark states or loosely bound hadronic molecules. Some theoretical models even propose that these states may arise solely from specific kinetic phenomena [11]. While the study of exotic states has been extensively pursued in particle physics over the past decades [12–16], their investigation in the context of heavy-ion collisions has recently garnered increased attention [17–22].

In the nucleus-nucleus collisions at the CERN Large Hadron Collider, the presence of a charm-rich deconfined medium offers a unique environment for studying the production of charmonium and other charmed states [23–31]. After the production from initial parton hard scatterings, these multicharm bound states are nearly melted in the extremely hot medium due to color screening and parton scatterings with thermal partons [32–34]. Consequently, the majority of experimentally measured multicharm particles are produced through the coalescence of charm quarks around the phase transition of the medium. The coalescence model has been employed to study the loosely bound objects such as light nuclei in heavy-ion collisions [35–38]. In the loosely bound states with a long formation time, coalescence models work as an effective model and neglect the details of the formation process but only consider the feature that the production of the formed states depends on their Wigner function and also the densities of the ingredient particles. The following interactions, such as the Coulomb interaction between the formed states and the medium, are also usually neglected, or this effect can be partially considered by assuming a later formation of the state.

The T_{cc}^{+} state, with a mass very close to the $D^{+}D^{*0}$ and $D^{0}D^{*+}$ thresholds [9,10], is regarded as a hadronic molecule with a weak binding energy in this study. Within this framework, charm quarks undergo energy loss in the deconfined medium and hadronize into D mesons during the hot medium's hadronization process. Subsequently, D mesons experience diffusion in the hadronic medium and can potentially combine with another D^{*} to form a weakly bound molecule. The coalescence probability between two D mesons depends

*Contact author: baoyi.chen@tju.edu.cn
†Contact author: yang_mm7@tju.edu.cn
‡Contact author: chen_ge2001@163.com
§Contact author: jzhao@subatech.in2p3.fr
‖Contact author: xiaohai.liu@tju.edu.cn

on their relative momentum, distance, and the wave function of T_{cc}^{+} [39–43]. This unique situation provides an opportunity to investigate properties related to the wave function of T_{cc}^{+}, which is crucial for understanding the nature of exotic particles. Moreover, the charm-rich environment significantly enhances the production of multicharm states, increasing the anticipation for experimental measurements in heavy-ion collisions. As coalescence models have been widely used to study the particle production including hadronic molecules in heavy-ion collisions [44–46], we employ the Langevin equation plus the coalescence model to study the energy loss of heavy quarks in the medium and also the production of multicharm states, like the hadronic state Ξ_{cc}^{++} and the molecular state T_{cc}^{+}. As both Ξ_{cc}^{++} and T_{cc}^{+} consist of two charm quarks, the difference between their production mainly comes from the different internal potential of the states.

The paper is structured as follows. Section II presents the dynamical equations governing the charm energy loss and the coalescence formula for the production of T_{cc}^{+} and Ξ_{cc}^{++}. Additionally, a brief overview of the evolution of the hot medium is provided. In Sec. III, the production of T_{cc}^{+} and Ξ_{cc}^{++} in heavy-ion collisions is plotted and thoroughly analyzed under various configurations. Finally, a conclusion is given in Sec. IV.

II. THEORETICAL MODEL

Heavy quarks have been found to exhibit a strong coupling with the deconfined medium that is generated in relativistic heavy-ion collisions [47–49]. By assuming small momentum transfer during each scattering event between charm quarks and thermal partons, it is possible to treat the trajectories of charm quarks in the medium as Brownian motion, a phenomenon that has been extensively studied using the Langevin equation [26,50,51]. Previous studies have indicated that heavy quarks experience energy loss in the quark-gluon plasma (QGP) through two distinct mechanisms. At low transverse momentum (p_T), the dominant contribution to energy loss for heavy quarks arises from elastic scatterings with thermal partons. Conversely, at high p_T, the energy loss of heavy quarks is primarily governed by medium-induced gluon radiation [52–59]. These two effects can be appropriately incorporated into the Langevin equation, which has been widely employed to investigate the dynamics of heavy quarks in the deconfined medium,

$$\frac{d\mathbf{p}}{dt} = -\eta(p)\mathbf{p} + \xi + \mathbf{f}_g, \tag{1}$$

where $\mathbf{p}$ is the three-momenta of charm quarks, and $\eta(p)$ is the drag coefficient. The momentum diffusion coefficient κ is determined through the fluctuation-dissipation relation, $\eta(p) = \kappa/(2TE)$. Here, T and $E = \sqrt{m_c^2 + p^2}$ represent the medium temperature and the energy of the charm quark, respectively, where the charm quark mass is defined as $m_c = 1.5$ GeV. The value of κ is determined by the spatial diffusion coefficient $\kappa\mathcal{D}_s = 2T^2$. Previous studies have extracted a value of $\mathcal{D}_s(2\pi T)$ to be approximately 5–7 in the QGP and larger in the hadronic medium [47,60]. In this study, we adopt the values of $\mathcal{D}_s(2\pi T) = 5$ in the QGP. In the hadronic medium, $\mathcal{D}_s(2\pi T)$ also varies with temperature ranging from 120 to 170 MeV. We approximate this variation by estimating a midpoint value of 8, like the cases in previous studies [19,27,51]. Assuming the random term ξ to be white noise, it satisfies the following correlation:

$$\langle \xi^i(t)\xi^j(t')\rangle = \kappa\delta^{ij}\delta(t-t'), \tag{2}$$

where $i, j = (1, 2, 3)$ represent three dimensions. For simplicity, the momentum dependence in the white noise term has been neglected. Besides random elastic collisions, heavy quarks also lose energy via gluon radiation. The force due to the gluon emission is defined as $\mathbf{f}_g = -d\mathbf{p}_g/dt$ with the gluon momentum $\mathbf{p}_g$. This contribution is absent for hadrons in the hadronic medium. When the time step is sufficiently small, the number of emitted gluons in the interval $t \sim t + dt$ can be considered as an emission probability [51,55],

$$P_{\rm rad}(t, dt) = \langle N_g(t, dt)\rangle = dt \int dx dk_T^2 \frac{dN_g}{dx dk_T^2 dt}. \tag{3}$$

Here, k_T represents the transverse momentum of the emitted gluon. The quantity $P_{\rm rad}$ can also be interpreted as the probability of emitting a single gluon within a time interval, with a value less than unity. Additionally, x denotes the ratio of the gluon energy to the heavy-quark energy. The spectrum of emitted gluons from massive quarks, $dN_g/dxdk_T^2dt$, is from the higher-twist calculation for the medium-induced gluon radiation in perturbative QCD [51].

Due to the large mass, heavy quarks are mainly produced via the initial parton hard scatterings, Therefore, the initial spatial distribution of heavy quarks is proportional to the density of nucleon binary collisions, which is the product of the two nuclear thickness functions, $dN_{c\bar{c}}/d\mathbf{x}_T \propto T_A(\mathbf{x}_T + \mathbf{b}/2)T_B(\mathbf{x}_T - \mathbf{b}/2)$. T_A and T_B are the thickness functions of two nuclei. $\mathbf{b}$ is the impact parameter. The initial momentum distribution of charm quarks is generated by the fixed-order plus next-to-leading log formula [61,62]. Then the initial position and the momentum of heavy quarks are generated via the Monte Carlo methods based on the above spatial and momentum distributions.

During the QGP phase transition at the critical temperature, charm quarks undergo hadronization, resulting in the formation of D mesons. For small transverse momentum (p_T), the hadronization process is described by the coalescence model, where charm quarks combine with thermal light quarks to form D mesons. On the other hand, at high p_T, the fragmentation process dominates the production of D mesons, with charm quarks emitting gluons. Since our focus is primarily on the total production of T_{cc}^{+}, mainly at low and intermediate p_T, we assume that all charm quarks hadronize into D mesons via the coalescence process. This approximation is valid for low and intermediate p_T. While for Ξ_{cc}^{++}, it consists of two charm quarks and one light quark, which is produced near the hadronization hypersurface [30]. The probability of heavy and light quarks turning into mesons and baryons is written

as [63]

$$\mathcal{P}_{c+\bar{q}\to D}(\mathbf{p}_D,\mathbf{x}_D)=\mathcal{H}_{c\to D}\int\frac{d\mathbf{p}_c d\mathbf{x}_c}{(2\pi)^3}\frac{d\mathbf{p}_{\bar{q}}}{(2\pi)^3}\frac{dN_c}{d\mathbf{p}_c d\mathbf{x}_c}\frac{dN_{\bar{q}}}{d\mathbf{p}_{\bar{q}}}f_D^W(\mathbf{p}_c,\mathbf{p}_{\bar{q}})\delta^{(3)}(\mathbf{p}_D-\mathbf{p}_c-\mathbf{p}_{\bar{q}}),\quad \delta^{(3)}(\mathbf{x}_D-\mathbf{x}_c), \tag{4}$$

$$\mathcal{P}_{c+c+q\to\Xi_{cc}}(\mathbf{p}_\Xi,\mathbf{x}_\Xi)=g_\Xi\int\frac{d\mathbf{p}_{c1}d\mathbf{x}_{c_1}}{(2\pi)^3}\frac{d\mathbf{p}_{c_2}d\mathbf{x}_{c_2}}{(2\pi)^3}\frac{d\mathbf{p}_q}{(2\pi)^3}\frac{dN_c}{d\mathbf{x}_{c_1}d\mathbf{p}_{c_1}}\frac{dN_c}{d\mathbf{x}_{c_2}d\mathbf{p}_{c_2}}\frac{dN_q}{d\mathbf{p}_q}f^W_{\Xi_{cc}^{++}}\left(\mathbf{p}_{c_1},\mathbf{p}_{c_2},\mathbf{p}_q,\mathbf{x}_{c_1},\mathbf{x}_{c_2}\right)$$
$$\times\,\delta^{(3)}\left(\mathbf{p}_\Xi-\mathbf{p}_{c_1}-\mathbf{p}_{c_2}-\mathbf{p}_q\right)\delta^{(3)}\left(\mathbf{x}_\Xi-\frac{m_{c_1}\mathbf{x}_{c_1}+m_{c_2q}\mathbf{x}_{c_2}}{m_{c_1}+m_{c_2q}}\right), \tag{5}$$

where the position $\mathbf{x}_D$ of the D meson is approximated as the position of charm quarks due to its large mass. $\mathbf{p}_c$ and $\mathbf{p}_q(\mathbf{p}_{\bar{q}})$ are the the momentum of the charm and light (antilight) quarks. The momentum conservation in the reaction is ensured by the presence of the δ function. So, the produced hadron is not on-shell. The on-shell process is accompanied by emitting other particles, such as photons, π, which are neglected firstly in this calculation. The quantity $dN_c/d\mathbf{p}_c d\mathbf{x}_c$ represents the distribution of charm quarks near the hadronization hypersurface, which is given by the Langevin equation. $dN_q/d\mathbf{p}_q$ (or $dN_{\bar{q}}/d\mathbf{p}_{\bar{q}}$) corresponds to the density of thermal light (antilight) quarks. In our calculation, the latter is usually modeled using a thermal distribution. In Eq. (4), the spatial part of the Wigner function has been integrated, since light quarks are abundant around charm quarks in QGP which means spatial conditions of the coalescence process can always be satisfied. So, the Wigner function is only momentum dependent, $f_D^W(\mathbf{p}_c,\mathbf{p}_{\bar{q}})=A\exp(-\sigma^2\mathbf{q}_r^2)$, where $\mathbf{q}_r=(E_c^{\rm cm}\mathbf{p}_c-E_{\bar{q}}^{\rm cm}\mathbf{p}_{\bar{q}})/(E_c^{\rm cm}+E_{\bar{q}}^{\rm cm})$ is the relative momentum between the charm quark and the light quark in their center-of-mass frame. $E_{c,\bar{q}}^{\rm cm}$ are the energy of two particles in their center-of-mass frame. The Gaussian width σ is related to the root-mean-square radius of the D meson through $\sigma^2=\frac{4}{3}\frac{(m_c+m_q)^2}{m_c^2+m_q^2}\langle r^2\rangle_D$, with $\sqrt{\langle r^2\rangle_D}=0.43$ fm [39,64]. The light quark mass is set to be $m=0.3$ GeV. A is a constant factor to make sure the coalescence probability equals 1 when the momentum of charm quark goes towards 0, $\mathbf{p}_c\to 0$. We force almost all charm quarks to form D mesons. Different from Ξ_{cc}^{++} as shown in Eq. (5), we use Eq. (4) to describe the coalescence process of D where we do not use the degeneracy factor for different D meson states instead of a hadronization fraction $\mathcal{H}_{c\to D}$. $\mathcal{H}_{c\to D}$ denotes the hadronization fraction of charm quarks transitioning into different states of D mesons, such as $D^{0,\pm}$, D^{*0}, and $D^{*\pm}$. These values can be estimated from the experimental data and thermal model [65–67], which are taken as $\mathcal{H}_{c\to D^0,D^+,D^{*0},D^{*+}}\approx(11.3\%,11.3\%,16.1\%,16.1\%)$. The rest of the fractions are to form other charmed hadrons, such as D_s, Λ_c, Ξ_c, and so on. The advantage of this way is to avoid considering all charmed hadrons and only focus on D mesons. This will increase the statistic effectively and it is proved the same as the way to consider all charmed hadrons separately [19].

For the case of Ξ_{cc}^{++}, it consists of two charm quarks and one light quark. The light quark is abundant around the charm quarks and with a small mass. In this case, one can assume that the coalescence probability of Ξ_{cc}^{++} mainly depends on the distributions of two charm quarks, and the three-body Wigner function can be simplified as the form of the two-body situation $c-cq$. Because charm quarks are rare particles in QGP, the spatial part of the Wigner function should be considered as well. The Wigner function of Ξ_{cc}^{++} can be expressed as $f^W_{\Xi_{cc}^{++}}=8\exp(-\mathbf{x}_r^2/\sigma^2)\exp(-\sigma^2\mathbf{q}_r^2)$, $\mathbf{x}_r=\mathbf{x}_{c_1}-\mathbf{x}_{c_2q}$ is the relative distance between the charm quark (c_1) and the charm-light pair (c_2q) in their center-of-mass frame, where the position of the charm-light pair is the same as the charm quark, $\mathbf{x}_{c_2q}=\mathbf{x}_{c_2}$. The Gaussian width σ is related to the root-mean-square radius of Ξ_{cc}^{++} through $\sigma^2=\frac{4}{3}\frac{(m_c+m_{cq})^2}{m_c^2+m_{cq}^2}\langle r^2\rangle_{\Xi_{cc}^{++}}$ and $\sqrt{\langle r^2\rangle_{\Xi_{cc}^{++}}}=0.5$ fm [30] in the following calculations. $m_{cq}=m_c+m_q$ is the mass of the charm-light pair. The spin and color degeneracy factor of Ξ_{cc}^{++} is extracted to be $g_{\Xi_{cc}^{++}}=1/54$.

In the hadronic medium, D mesons continue to undergo diffusion until the kinetic freeze-out stage. Since the binding energy of the T_{cc}^+ molecule is considered to be small, T_{cc}^+ is produced at temperatures close to the kinetic freeze-out temperature. We also adopt a Gaussian form for the Wigner function of T_{cc}^+, given by $f^W_{T_{cc}^+}=8\exp(-\mathbf{x}_r^2/\sigma^2)\exp(-\sigma^2\mathbf{q}_r^2)$ [39]. Here, $\mathbf{x}_r$ and $\mathbf{q}_r$ denote the relative distance and the relative momentum between the D meson and the D^* meson, respectively. To study the production of T_{cc}^+ in the hadronic medium, we consider different values for the root-mean-square radius of T_{cc}^+, which carries information about the T_{cc}^+ wave function. In nucleus-nucleus collisions, the parton densities of nucleons in the nucleus can be modified by cold nuclear matter effects, such as the shadowing effect. This can also impact the initial distributions of charm quarks. The shadowing factor is calculated using the EPS09 package and is applied directly to the aforementioned initial distribution of charm quarks. Furthermore, the gluons can undergo scattering with other nucleons, resulting in additional energy before fusing into a charm pair. This additional energy is transferred to the charm quarks and modifies their initial momentum distributions. Since charm quarks experience significant energy loss in the quark-gluon plasma, we neglect the modification of the Cronin effect on the initial distribution of charm quarks in this study.

The deconfined matter generated in relativistic heavy-ion collisions exhibits properties similar to those of a nearly perfect fluid [68,69]. The evolution of the hot medium can be effectively simulated using hydrodynamic equations [69–72]. We employ the MUSIC package [70,73] to simulate the dynamical evolutions of the deconfined medium and the hadronic gas. For the equation of state (EoS) of the medium, we employ

the EoS parametrized with the lattice EoS at zero baryon density from the HotQCD Collaboration and the hadron resonance gas EoS [74,75]. There is a crossover phase transition between two phases [76]. We specify a critical temperature $T_c = 170$ MeV, above and below which the medium is treated as deconfined and confined, respectively. The initial conditions of the hot medium and the starting time of hydrodynamic evolutions are determined based on the final spectrum of light hadrons [77].

III. T_{cc} PRODUCTION IN HEAVY-ION COLLISIONS

As T_{cc}^+ is considered to be a bound state of D and D^* mesons, its production can be significantly enhanced in nuclear collisions due to the large number of charm quarks involved. Since experiments only measured T_{cc}^+, we take the isospin to be 0 and calculate the production of this specific state via the coalescence of $D^{+/0}D^{*0/*+}$. The production cross section of the charm pair has been experimentally measured. In the central rapidity proton-proton (pp) collision at a center-of-mass energy of $\sqrt{s_{NN}} = 5.02$ TeV, the rapidity-differential cross section is $d\sigma_{pp}/dy = 1.165$ mb [66]. The production of T_{cc}^+ depends on both the phase-space distribution of D mesons and the Wigner function of T_{cc}^+ . The positions and momenta of $D^{0/+}$, $D^{*0/*+}$ before the coalescence of T_{cc}^+ are determined using the Langevin equation. The Wigner function, which is related to the T_{cc}^+ wave function, is approximated as a Gaussian function with a width determined by the root-mean-square radius $\sqrt{\langle r^2\rangle}$. Considering that the binding energy of T_{cc}^+ is very small, it can be easily dissociated by hadronic scatterings in the hadron gas. We assume that the loosely bound molecule is produced at a low temperature close to the kinetic freeze-out temperature of the medium, and we take different values of $\sqrt{\langle r^2\rangle}$ into the calculation due to the uncertainty of the T_{cc}^+ wave function.

To get an estimation of the root-mean-radius of T_{cc}^+ states, the DD^* potentials are studied within the framework of heavy-meson chiral effective field theory. The effective potentials of the DD^* system from the contact and one-pion exchange (OPE) diagrams at the leading order are considered. The contact terms mainly affect the short-range interaction between particles while the OPE contribution determines the behavior of the long-range interaction. Both the contact and the OPE interaction are isospin I dependent, where I is the isospin of the formed molecular state. The contact terms lead to the attractive interaction in the $I = 0$ channel while the repulsive interaction is in the $I = 1$ channel. The OPE interaction is attractive in both cases. So, the total potential in the short distance for the $I = 1$ channel is repulsive but for the $I = 0$ channel is attractive (see detail in Ref. [78]). In this study, we only consider the $I = 0$ channel, which has the attractive potential and supports the formation of the molecular state. The potential in the momentum can be shown as

$$V_{\rm contact}(q) = -2D_a - 2D_b + 6E_a + 6E_b,$$
$$V_{\rm OPE}(q) = -\frac{g^2}{4f_\pi^2}\frac{q^2}{q^2 + m_\pi^2}. \quad (6)$$

TABLE I. The binding energy (B.E.) and average radius $\langle r\rangle$ of molecule T_{cc}^+ states with different cutoff parameter Λ in potential.

Λ	0.66	0.68	0.7	0.75	0.8	0.9	1.0
B.E. (keV)	0.03	0.3	0.8	2.61	5.9	17.7	38.4
$\langle r\rangle$ (fm)	5.04	3.87	2.94	1.74	1.26	0.83	0.62

We take the same parameters as Ref. [78], $D_a = -6.62$ $E_a = -5.74$ and $D_b = E_b = 0$. The coupling constant $g = 0.65$ and $f_\pi = 86$ MeV. $m_\pi = 135$ MeV is the π mass. The potential in coordinate space can be obtained via transformation. We introduce the monopole-type form factor at each vertex to take into account the size effect of $D^{(*)}$ mesons:

$$F(q) = \left(\frac{\Lambda^2 - m^2}{\Lambda^2 + q^2}\right)^2. \quad (7)$$

The cutoff parameter Λ is determined from the size of $D^{(*)}$ and is usually taken around 1 GeV. Solving the two-body Schrödinger equation with this potential, we can get the wave function and the binding energy of the D^0D^{*0} bound state, as shown in Table I and Fig. 1. Our results are consistent with other studies with many other vector meson exchange potentials [79,80].

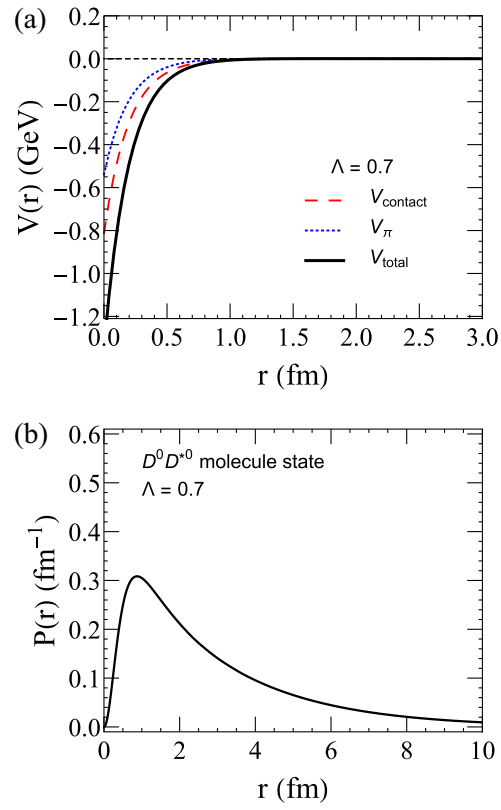

FIG. 1. (a) The total potential between D^0 and D^{*0}. (b) The radial probability $P(r) = |\psi(r)|^2 r^2$ of the loosely bound molecular state T_{cc}^+.

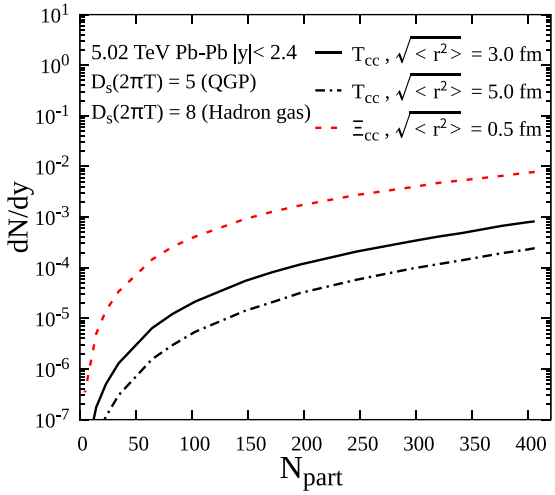

FIG. 2. The T_{cc}^{+} production, measured by dN/dy as a function of the number of participants $N_{\rm part}$ is presented for central rapidity in Pb-Pb collisions at $\sqrt{s_{NN}} = 5.02$ TeV. We select a coalescence temperature of $T_{\rm coal} = 0.12$ GeV [19,81]. Two typical values for the root-mean-square radius of T_{cc}, representing different binding strengths, are considered as $\sqrt{\langle r^2\rangle} = (3.0, 5.0)$ fm. The spatial diffusion coefficients for charm quarks and D mesons are chosen as $\mathcal{D}_s(2\pi T) = 5$ and 8, respectively, in the QGP and the hadronic medium. The red dashed line represents the hadronic state Ξ_{cc}^{++} as a comparison, which is produced near the hadronization hypersurface of the QGP medium.

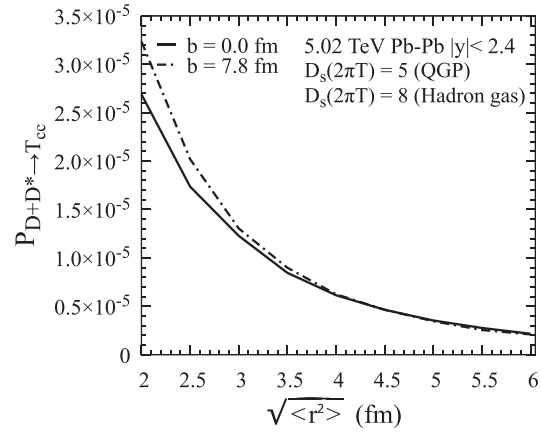

FIG. 3. The coalescence probability between one D meson and one D^* meson to form T_{cc}^{+} varies with the root-mean-square radius $\sqrt{\langle r^2\rangle}$ of T_{cc}^{+} in the central rapidity of $\sqrt{s_{NN}} = 5.02$ TeV Pb-Pb collisions. Two collision centralities are selected with the impact parameters to be $b = 0$ and 7.8 fm (minimum bias collisions). The coalescence temperature of the T_{cc}^{+} production is $T_{\rm coal} = 0.12$ GeV.

Figure 2 displays the production of T_{cc}^{+} and Ξ_{cc}^{++} for various collision centralities. The production of T_{cc}^{+} is directly proportional to the densities of D and D^* mesons, which increase as one moves from peripheral to central collisions. This leads to an enhanced T_{cc}^{+} production compared to that in proton-proton (pp) collisions. We consider T_{cc}^{+} production with different root-mean-square radii, which represent varying binding strengths of T_{cc}^{+} . As the value of the root-mean-square radius decreases, a larger number of D and D^* mesons, with even larger relative momentum, can effectively combine to form the T_{cc}^{+} molecular state. The production of T_{cc}^{+} exhibits an increase of approximately 3.5 times when the value of the root-mean-square radius ($\sqrt{\langle r^2\rangle}$) varies from 5.0 to 3.0 fm, indicating a stronger binding scenario for T_{cc}^{+}. The ultimate production of T_{cc}^{+} is influenced by the selection of T_{cc}^{+} geometry size. This feature renders our model well-suited for extracting information about T_{cc}^{+} through its final production in heavy-ion collisions. In peripheral collisions, both the volume of the QGP and the number of charm pairs are significantly reduced, resulting in a suppression of T_{cc}^{+} production from the coalescence process. The total production of T_{cc}^{+} is predominantly governed by the primordial production, similar to the case of J/ψ. We also study the production of Ξ_{cc}^{++}, which also consists of two charm quarks and has been regarded as a hadronic state. Due to the strong binding potential, its production becomes around 10 times larger than the molecular T_{cc}^{+} (see the red dashed line in Fig. 2). In our theoretical calculations in Fig. 2, where we have not considered the primordial production, the T_{cc}^{+} production is underestimated at the small $N_{\rm part}$. However, for the large $N_{\rm part}$ corresponding to central collisions, the extremely hot medium dissociates almost all of the charmed hadrons, making the coalescence model a suitable approach to describe the production of charmed particles.

To investigate the influence of the binding strength of T_{cc}^{+} on its production, we calculate the coalescence probability between one randomly generated D meson and one randomly generated D^* meson in the hot medium. The results are shown in Fig. 3. As the value of $\sqrt{\langle r^2\rangle}$ increases, indicating a weaker binding strength of T_{cc}^{+}, the momentum part of the coalescence probability of D and D^* decreases due to the presence of $\exp(-\sigma^2 q_r^2)$ in the Wigner function. However, the coalescence probability increases in the spatial part, characterized by $\exp(-x_r^2/\sigma^2)$. Two parts are connected, and the combined effect results in a significant suppression of the coalescence probability $P_{D+D^*\to T_{cc}}$ with the increasing $\sqrt{\langle r^2\rangle}$, as demonstrated in Fig. 3. We consider two collision centralities, namely, the most central collisions and the minimum-bias collisions, which correspond to the production of two different volumes of the QGP. When the value of $\sqrt{\langle r^2\rangle}$ is small, the coalescence probability $P_{D+D^*\to T_{cc}}$ depends on the diffusions of charm quarks and D mesons in the expanding medium. In scenarios where the medium expansion is more intense and persists for a longer duration, such as in the case of $b = 0$, D and D^* mesons experience greater diffusion and spread out over a larger volume. Consequently, the coalescence probability between a D meson and a D^* meson is reduced when the geometry size of T_{cc}^{+} is smaller. However, as $\sqrt{\langle r^2\rangle}$ increases, D and D^* mesons that are farther apart can also combine to form T_{cc}^{+} . This feature results in the coalescence probability $P_{D+D^*\to T_{cc}}$ being less sensitive to the volume of the QGP, as observed in the cases of the QGP generated in the most central ($b = 0$) and minimum-bias collisions, as shown by the two lines in Fig. 3.

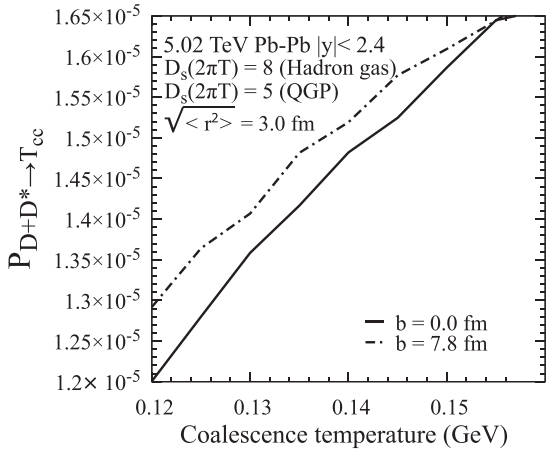

FIG. 4. The coalescence probability $P_{D+D^*\to T_{cc}}$ between one D meson and one D^* meson to form T_{cc}^+ varies with the coalescence temperature of T_{cc}^+ . The impact parameters are selected as $b = 0$ and $b = 7.8$ fm, respectively, which correspond to the most-central collisions and the minimum-bias collisions. The root-mean-square radius used in the Wigner function of T_{cc}^+ is selected as $\sqrt{\langle r^2\rangle} = 3.0$ fm.

When the binding energies of T_{cc}^+ become different, the corresponding coalescence temperatures should also differ. In Fig. 4, we calculated the coalescence probability between one D meson and one D^* meson at different hypersurfaces specified with the coalescence temperature $T_{\rm coal}$. The hot medium is chosen in the most central collisions at 5.02-TeV Pb-Pb collisions. The root-mean-square radius is $\sqrt{\langle r^2\rangle} = 3.0$ fm. When $\sqrt{\langle r^2\rangle}$ is large (such as $\sqrt{\langle r^2\rangle} \geqslant 3$ fm), the value of $P_{D+D^*\to T_{cc}}$ depends less on the volume of the hot medium at different collision centralities. Therefore, we only consider one collision centrality in Fig. 4. In the expanding hot medium, when the coalescence temperature varies from 0.12 to 0.16 GeV, the distance between one D meson and one D^* meson becomes shorter as they move to the regions satisfying the coalescence temperature, which increases the coalescence probability between D and D^*. The value of $P_{D+D^*\to T_{cc}}$ increases by around 40% when $T_{\rm coal}$ changes from 0.12 to 0.16 GeV.

IV. SUMMARY

We utilize the Langevin equation plus the coalescence model to investigate the dynamical evolution of charm quarks in the quark-gluon plasma and D mesons in the hadronic medium, as well as the production of T_{cc}^+ through the combination of D and D^* mesons. The production of T_{cc}^+ is closely linked to the phase-space densities of D mesons at the coalescence hypersurface, which are obtained from the Langevin equation, and the Wigner function, which is related to the wave function of T_{cc}^+ . To elucidate the properties of T_{cc}^+, we consider different binding energies by employing different Wigner functions to calculate the T_{cc}^+ production. Since the phase-space distributions of D mesons are typically determined by fitting the observables of D mesons in heavy-ion collisions, the uncertainty in T_{cc}^+ production mainly arises from the Wigner function at finite temperatures. Therefore, we vary the width of the Wigner function and the coalescence temperatures to study the production of molecular T_{cc}^+ in different centralities of $\sqrt{s_{NN}} = 5.02$ TeV Pb-Pb collisions. Ξ_{cc}^{++} is also calculated as a comparison. Its production becomes larger than the molecular T_{cc}^+ due to the large binding energies of Ξ_{cc}^{++} reflected in the width of the Wigner function. For T_{cc}^+, when the wave function becomes broader corresponding to a weaker binding strength, the coalescence probability between D and D^* to form T_{cc}^+ is reduced evidently. When the coalescence temperature increases, T_{cc}^+ is produced at an earlier stage of the hot medium, where the spatial density of D mesons is higher, thereby enhancing the T_{cc}^+ production. The production of T_{cc}^+ is sensitive to the details of the Wigner function. This characteristic makes our model particularly suitable for exploring the information about T_{cc}^+ through its final production and investigating the properties of exotic states containing multiple charm quarks.

ACKNOWLEDGMENTS

This work is supported by the National Natural Science Foundation of China (NSFC) under Grants No. 12175165, No. 11975165, and No. 12235018. J.Z. is supported by the European Union's Horizon 2020 research and innovation program under Grant Agreement No. 824093 (STRONG-2020).

[1] H. X. Chen, W. Chen, X. Liu, and S. L. Zhu, Phys. Rep. **639**, 1 (2016).
[2] Y. R. Liu, H. X. Chen, W. Chen, X. Liu, and S. L. Zhu, Prog. Part. Nucl. Phys. **107**, 237 (2019).
[3] Y. Dong, A. Faessler, and V. E. Lyubovitskij, Prog. Part. Nucl. Phys. **94**, 282 (2017).
[4] F. S. Navarra, M. Nielsen, and S. H. Lee, Phys. Lett. B **649**, 166 (2007).
[5] E. Braaten, L. P. He, and A. Mohapatra, Phys. Rev. D **103**, 016001 (2021).
[6] E. J. Eichten and C. Quigg, Phys. Rev. Lett. **119**, 202002 (2017).
[7] J. Zhao, S. Shi, and P. Zhuang, Phys. Rev. D **102**, 114001 (2020).
[8] G. Huang, J. Zhao, and P. Zhuang, Phys. Rev. D **103**, 054014 (2021).
[9] R. Aaij *et al.* (LHCb Collaboration), Nat. Phys. **18**, 751 (2022).
[10] R. Aaij *et al.* (LHCb Collaboration), Nat. Commun. **13**, 3351 (2022).
[11] F. K. Guo, C. Hanhart, Ulf-G. Meißner, Q. Wang, Q. Zhao, and B.-S. Zou, Rev. Mod. Phys. **90**, 015004 (2018); **94**, 029901(E) (2022).
[12] D. Acosta *et al.* (CDF Collaboration), Phys. Rev. Lett. **93**, 072001 (2004).
[13] C. Bignamini, B. Grinstein, F. Piccinini, A. D. Polosa, and C. Sabelli, Phys. Rev. Lett. **103**, 162001 (2009).
[14] N. Brambilla, S. Eidelman, C. Hanhart, A. Nefediev, C. P. Shen, C. E. Thomas, A. Vairo, and C. Z. Yuan, Phys. Rep. **873**, 1 (2020).
[15] E. Braaten, L.-P. He, K. Ingles, and J. Jiang, Phys. Rev. D **106**, 034033 (2022).

[16] S. Cho and S. H. Lee, Phys. Rev. C **101**, 024902 (2020).
[17] A. Esposito, E. G. Ferreiro, A. Pilloni, A. D. Polosa, and C. A. Salgado, Eur. Phys. J. C **81**, 669 (2021).
[18] E. Braaten, L. P. He, K. Ingles, and J. Jiang, Phys. Rev. D **103**, L071901 (2021).
[19] B. Chen, L. Jiang, X. H. Liu, Y. Liu, and J. Zhao, Phys. Rev. C **105**, 054901 (2022).
[20] Y. Hu, J. Liao, E. Wang, Q. Wang, H. Xing, and H. Zhang, Phys. Rev. D **104**, L111502 (2021).
[21] H. Yun, D. Park, S. Noh, A. Park, W. Park, S. Cho, J. Hong, Y. Kim, S. Lim, and S. H. Lee, Phys. Rev. C **107**, 014906 (2023).
[22] B. Wu, X. Du, M. Sibila, and R. Rapp, Eur. Phys. J. A **57**, 122 (2021); **57**, 314(E) (2021).
[23] A. Andronic, P. Braun-Munzinger, K. Redlich, and J. Stachel, Phys. Lett. B **571**, 36 (2003).
[24] L. Yan, P. Zhuang, and N. Xu, Phys. Rev. Lett. **97**, 232301 (2006).
[25] X. Du, M. He, and R. Rapp, Phys. Rev. C **96**, 054901 (2017).
[26] B. Chen and J. Zhao, Phys. Lett. B **772**, 819 (2017).
[27] B. Chen, L. Wen, and Y. Liu, Phys. Lett. B **834**, 137448 (2022).
[28] B. Wu, Z. Tang, M. He, and R. Rapp, Phys. Rev. C **109**, 014906 (2024).
[29] J. Zhao and P. Zhuang, Few-Body Syst. **58**, 100 (2017).
[30] J. Zhao, H. He, and P. Zhuang, Phys. Lett. B **771**, 349 (2017).
[31] V. Minissale, S. Plumari, Y. Sun, and V. Greco, Eur. Phys. J. C **84**, 228 (2024).
[32] H. Satz, J. Phys. G: Nucl. Part. Phys. **32**, R25 (2006).
[33] N. Brambilla, J. Ghiglieri, A. Vairo, and P. Petreczky, Phys. Rev. D **78**, 014017 (2008).
[34] L. Wen and B. Chen, Phys. Lett. B **839**, 137774 (2023).
[35] J. Gosset, H. H. Gutbrod, W. G. Meyer, A. M. Poskanzer, A. Sandoval, R. Stock, and G. D. Westfall, Phys. Rev. C **16**, 629 (1977).
[36] B. I. Abelev *et al.* (STAR Collaboration), Science **328**, 58 (2010).
[37] C. Adler *et al.* (STAR Collaboration), Phys. Rev. Lett. **87**, 262301 (2001); **87**, 279902(E) (2001).
[38] P. Braun-Munzinger and B. Dönigus, Nucl. Phys. A **987**, 144 (2019).
[39] V. Greco, C. M. Ko, and R. Rapp, Phys. Lett. B **595**, 202 (2004).
[40] S. Cho, K. J. Sun, C. M. Ko, S. H. Lee, and Y. Oh, Phys. Rev. C **101**, 024909 (2020).
[41] R. Rapp and H. van Hees, Heavy quarks in the quark-gluon plasma, in *Quark-Gluon Plasma 4*, edited by R. C. Hwa and X.-N. Wang (World Scientific, Singapore, 2010), pp. 111–206.
[42] S. Cho *et al.* (ExHIC Collabaoration), Phys. Rev. Lett. **106**, 212001 (2011).
[43] A. Andronic, P. Braun-Munzinger, M. K. Köhler, K. Redlich, and J. Stachel, Phys. Lett. B **797**, 134836 (2019).
[44] S. Cho *et al.* (ExHIC Collaboration), Prog. Part. Nucl. Phys. **95**, 279 (2017).
[45] S. Cho *et al.* (ExHIC Collaboration), Phys. Rev. C **84**, 064910 (2011).
[46] L. M. Abreu, H. P. L. Vieira, and F. S. Navarra, Phys. Rev. D **105**, 116029 (2022).
[47] M. He, R. J. Fries, and R. Rapp, Phys. Rev. Lett. **110**, 112301 (2013).
[48] D. Banerjee, S. Datta, R. Gavai, and P. Majumdar, Phys. Rev. D **85**, 014510 (2012).
[49] H. T. Ding, F. Karsch, and S. Mukherjee, Int. J. Mod. Phys. E **24**, 1530007 (2015).
[50] M. He, R. J. Fries, and R. Rapp, Phys. Rev. C **86**, 014903 (2012).
[51] S. Cao, G. Y. Qin, and S. A. Bass, Phys. Rev. C **92**, 024907 (2015).
[52] M. Gyulassy, P. Levai, and I. Vitev, Phys. Rev. Lett. **85**, 5535 (2000).
[53] X. f. Guo and X. N. Wang, Phys. Rev. Lett. **85**, 3591 (2000).
[54] U. A. Wiedemann, Nucl. Phys. A **690**, 731 (2001).
[55] B. W. Zhang, E. Wang, and X. N. Wang, Phys. Rev. Lett. **93**, 072301 (2004).
[56] G. Y. Qin, J. Ruppert, C. Gale, S. Jeon, G. D. Moore, and M. G. Mustafa, Phys. Rev. Lett. **100**, 072301 (2008).
[57] S. A. Bass, C. Gale, A. Majumder, C. Nonaka, G. Y. Qin, T. Renk, and J. Ruppert, Phys. Rev. C **79**, 024901 (2009).
[58] N. Armesto, B. Cole, C. Gale, W. A. Horowitz, P. Jacobs, S. Jeon, M. van Leeuwen, A. Majumder, B. Muller, G. Y. Qin *et al.*, Phys. Rev. C **86**, 064904 (2012).
[59] A. Majumder and M. Van Leeuwen, Prog. Part. Nucl. Phys. **66**, 41 (2011).
[60] R. Rapp, P. B. Gossiaux, A. Andronic, R. Averbeck, S. Masciocchi, A. Beraudo, E. Bratkovskaya, P. Braun-Munzinger, S. Cao, A. Dainese *et al.*, Nucl. Phys. A **979**, 21 (2018).
[61] M. Cacciari, M. Greco, and P. Nason, J. High Energy Phys. 05 (1998) 007.
[62] M. Cacciari, S. Frixione, N. Houdeau, M. L. Mangano, P. Nason, and G. Ridolfi, J. High Energy Phys. 10 (2012) 137.
[63] W. Zhao, C. M. Ko, Y. X. Liu, G. Y. Qin, and H. Song, Phys. Rev. Lett. **125**, 072301 (2020).
[64] J. Zhao, K. Zhou, S. Chen, and P. Zhuang, Prog. Part. Nucl. Phys. **114**, 103801 (2020).
[65] S. Acharya *et al.* (ALICE Collaboration), J. High Energy Phys. 10 (2018) 174.
[66] S. Acharya *et al.* (ALICE Collaboration), Phys. Rev. D **105**, L011103 (2022).
[67] J. Zhao, J. Aichelin, P. B. Gossiaux, V. Ozvenchuk, and K. Werner, arXiv:2401.17096.
[68] T. Hirano and M. Gyulassy, Nucl. Phys. A **769**, 71 (2006).
[69] H. Song, S. A. Bass, U. Heinz, T. Hirano, and C. Shen, Phys. Rev. Lett. **106**, 192301 (2011); **109**, 139904(E) (2012).
[70] B. Schenke, S. Jeon, and C. Gale, Phys. Rev. Lett. **106**, 042301 (2011).
[71] L. Pang, Q. Wang, and X. N. Wang, Phys. Rev. C **86**, 024911 (2012).
[72] C. Shen, Z. Qiu, H. Song, J. Bernhard, S. Bass, and U. Heinz, Comput. Phys. Commun. **199**, 61 (2016).
[73] B. Schenke, S. Jeon, and C. Gale, Phys. Rev. C **82**, 014903 (2010).
[74] J. E. Bernhard, J. S. Moreland, S. A. Bass, J. Liu, and U. Heinz, Phys. Rev. C **94**, 024907 (2016).
[75] A. Bazavov *et al.* (HotQCD Collaboration), Phys. Rev. D **90**, 094503 (2014).
[76] A. Bazavov, T. Bhattacharya, M. Cheng, C. DeTar, H. T. Ding, S. Gottlieb, R. Gupta, P. Hegde, U. M. Heller, F. Karsch *et al.*, Phys. Rev. D **85**, 054503 (2012).
[77] W. Zhao, H.-j. Xu, and H. Song, Eur. Phys. J. C **77**, 645 (2017).

[78] H. Xu, B. Wang, Z.-W. Liu, and X. Liu, Phys. Rev. D **99**, 014027 (2019); H. Xu, B. Wang, Z. W. Liu, and X. Liu, **104**, 119903(E) (2021).
[79] N. Li, Z. F. Sun, X. Liu, and S. L. Zhu, Phys. Rev. D **88**, 114008 (2013).
[80] S. Ohkoda, Y. Yamaguchi, S. Yasui, K. Sudoh, and A. Hosaka, Phys. Rev. D **86**, 034019 (2012).
[81] H. Song and U. W. Heinz, Phys. Rev. C **78**, 024902 (2008).